Journal of Technology and Social Science (JTSS)

Propagation of Stress Waves in Viscoelastic Rods and Plates (3)
- Acoustic Impedance of a Viscoelastic Rod : the Applicability to the Inverse Calculations -

Ryuzo Horiguchi[1,a] and Takao Yamaguchi[2,b]

[1]Processing Development Research Laboratories, Kao Corporation, 2-1-3, Bunka, Sumidaku, Tokyo 131-8501, Japan

[2]Faculty of Science and Technology, Gunma University, 1-5-1 Tenjincho, Kiryu 376-8515, Japan

[a]<horiguchi.ryuuzou@kao.com>, [b]<yamagme3@gunma-u.ac.jp>,

Keywords: acoustic impedance, rod, viscoelastic, inversion

Abstract. We had derived the explicit analytical expression of the complex wave number of a longitudinal wave in a viscoelastic rod and a flexural wave in a viscoelastic beam. In this study, we deal with the longitudinal waves in viscoelastic rods such as cork. This paper focuses on the inverse analysis method to identify the viscoelasticity of a specimen using the acoustic impedance of a viscoelastic rod obtained from the experiment. This method consists of inverse calculations for each step of the physical model. With our simple inverse formulas, it is possible to obtain the complex wave number from the characteristic impedance. It is also possible to identify viscoelasticity from the complex wave number. Furthermore, we developed an inverse calculation method to identify the characteristic impedance of the specimen from the acoustic impedance after the specimen. We confirmed that the conditions of direct analysis are reproduced by inverse analysis.

1. Introduction

Among shock-absorbing and sound-absorbing materials, cork behaves as a homogeneous viscoelastic body without breathability. Policarpo et al. [1] hammer-excited a cork specimen sandwiched between steel rods on both sides. They identified the storage modulus and loss factor of the cork specimen for each eigenmode from the frequency response function.

We have studied stress waves propagating in viscoelastic rods, beams, and plates [3], [4]. In the previous study [4], we calculated the acoustic impedance of a cork rod using our formulas of the complex wave number. The calculated results were validated via a comparison with the data of Policarpo et al. [1].

Many studies have identified the physical properties of a specimen from acoustic impedance. However, many of them are problems of mathematical scattering. Mouhtadi et al. [2] irradiated ultrasonic waves onto plates such as polyethylene to identify the mass density, elastic modulus of the specimen, and attenuation constants in the specimen and air. In their study, the acoustic impedance between the transmitter and the receiver was used for identifying the physical properties. However, they assumed that the attenuation constants in the material and in air are proportional to the first and second powers of the frequency, respectively.

Furthermore, we have studied an inverse analysis method for determining viscoelasticity from the acoustic impedance of a viscoelastic rod. Our study aims at low frequencies below several kilohertz. We use the explicit formulas expressing the complex wave number (real wave number and attenuation constant) for given viscoelasticity (storage modulus and loss factor) [3]. Our formulas are based on the wave propagation in viscoelastic rods and plates, and we do not assume linear and quadratic frequency dependence.

In this paper, we show the inverse analysis method for obtaining viscoelasticity when the acoustic impedance of the system is obtained. Each step of the inverse analysis traces the steps of direct analysis in reverse.

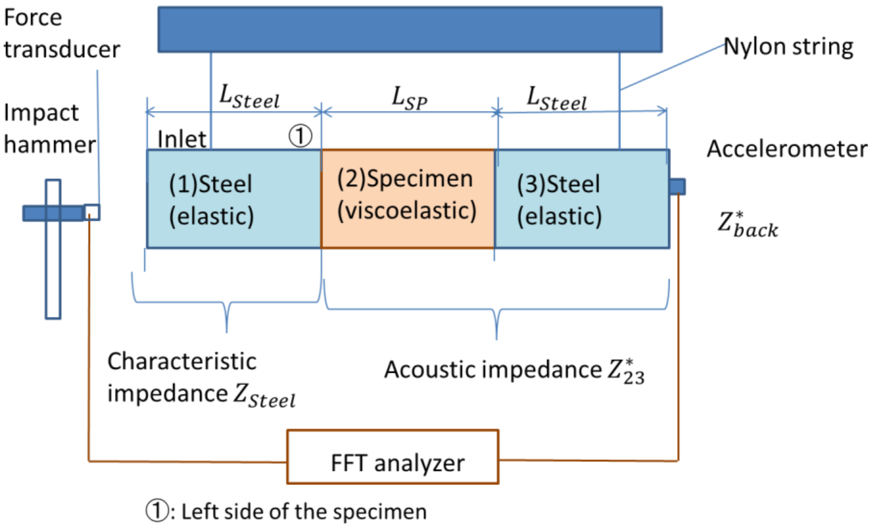

Fig.1. Experimental setup of Policarpo et al. [1]

2. Applicability to the Inverse Calculations - Estimation of Viscoelasticity from Acoustic Impedance

In our previous study [4], we calculated the complex wave number (real wave number and attenuation constant (factor)) using the viscoelastic data estimated by Policarpo et al.[1] Subsequently, we calculated the acoustic impedance from the complex wave number.

The acoustic impedance of the whole system Z^*_{tot} in Fig. 1 can be calculated from the frequency response function of Policarpo et al. [4]

For Fig. 1, the acoustic impedance of the whole system and the specimen can be expressed as follows [4]:

$$\frac{Z^*_{tot}}{Z_{Steel}} = \frac{\left(Z^*_{23}/Z_{Steel}\right) + i\tan\left(\omega L_{Steel}/c_{Steel}\right)}{1 + i\left(Z^*_{23}/Z_{Steel}\right)\tan\left(\omega L_{Steel}/c_{Steel}\right)}, i = \sqrt{-1}$$

where (1)

$$Z_{Steel} = \rho_{Steel} c_{Steel}, \; c_{Steel} = \sqrt{\frac{E_{Steel}\left(1-\nu_{Steel}\right)}{\rho_{Steel}\left(1+\nu_{Steel}\right)\left(1-2\nu_{Steel}\right)}}$$

$$Z^*_{23} = Z^*_{SP} \cdot \frac{1 + \frac{Z^*_{SP}}{Z^*_3}\tanh\left[(\alpha + i\beta)L_{SP}\right]}{\frac{Z^*_{SP}}{Z^*_3} + \tanh\left[(\alpha + i\beta)L_{SP}\right]} = Z^*_{SP} \cdot \frac{\coth\left[(\alpha + i\beta)L_{SP}\right] + \frac{Z^*_{SP}}{Z^*_3}}{1 + \frac{Z^*_{SP}}{Z^*_3}\coth\left[(\alpha + i\beta)L_{SP}\right]}, \quad (2)$$

$$Z^*_{SP} = \frac{\rho\omega(\beta + i\alpha)}{\beta^2 + \alpha^2},$$

where

ω : Radial frequency [rad/s], ρ : mass density of the specimen $[kg/m^3]$,

β and α : Real wave number and attenuation constant in the specimen, respectively (Eqs. (5) and (6)),

Z^*_{23} : Acoustic impedance as viewed from the left end of the specimen $[Pa \cdot s/m]$,

Z^*_{SP}: Characteristic impedance of the specimen $[Pa \cdot s/m]$,

L_{SP}: Length of the specimen [m],

Z_{Steel} : Characteristic impedance of the steel rod $[Pa \cdot s/m]$,

c_{Steel}: Phase velocity in steel [m/s], ρ_{Steel} : mass density of steel $[kg/m^3]$,

ν_{Steel}: Poisson's ratio of steel [-], L_{Steel}: Length of the steel rod [m],

$$Z_3^* = Z_{3b}^* \approx iZ_{Steel} \tan\left(\omega L_{Steel}/c_{Steel}\right) \tag{3}$$

: Acoustic impedance viewed from the left end of the rightmost steel rod $[Pa \cdot s/m]$,

Relations between hyperbolic functions

$$\coth[(\alpha + i\beta)L_{SP}] = [\sinh(2\alpha L_{SP}) - i\sin(2\beta L_{SP})]/[\cosh(2\alpha L_{SP}) - \cos(2\beta L_{SP})]. \tag{4}$$

Real Wave Number [1/m]

$$\beta(\omega) = \omega\left[\frac{\rho}{2E'(\omega)}\right]^{\frac{1}{2}}\left[\frac{1}{\left(1+\tan^2\delta\right)^{1/2}} + \frac{1}{1+\tan^2\delta}\right]^{\frac{1}{2}} \tag{5}$$

Attenuation Constant [1/m]

$$\alpha(\omega) = \omega\left[\frac{\rho}{2E'(\omega)}\right]^{\frac{1}{2}}\left[\frac{1}{\left(1+\tan^2\delta\right)^{1/2}} - \frac{1}{1+\tan^2\delta}\right]^{\frac{1}{2}}, \tag{6}$$

where

$E'(\omega)$: Storage modulus of the specimen [Pa],

$\tan\delta$: loss tangent (loss factor) of the specimen[-].

In this study, we investigate the inverse method for obtaining viscoelasticity when the acoustic impedance of the system is obtained. Each step of the inverse analysis traces the steps of direct analysis in reverse. We examined the inverse analysis method divided step by step as follows:

(a) Estimation of acoustic impedance Z_{23}^* from acoustic impedance Z_{tot}^*.

(Z_{23}^* and Z_{tot}^* : acoustic impedance viewed from the left end of the specimen and from the left end of the whole system)

(b) Estimation of the characteristic impedance Z_{SP}^* of the specimen from the acoustic impedance Z_{23}^*

(c) Estimation of viscoelasticity $(E', tan\delta)$ of the specimen from the characteristic impedance Z_{SP}^* (See Appendix A)

In this section, each inversion step is confirmed via numerical calculation. We start with a simple procedure and confirm the validity via numerical calculation.

2.1 Relationship between Complex Wave Number, Viscoelasticity, and Characteristic Impedance -Numerical Calculation of the Direct and Inverse Analysis -

For a longitudinal wave propagating in a viscoelastic rod, there are simple one-to-one relations between complex elastic modulus, complex wave number, and characteristic impedance (See Appendix B).

Figure 2 shows the relationship between viscoelasticity and complex wave number. In Fig.2, numerical examples are shown as "(Direct)" and "(Inverse)." In the direct calculation, when the storage modulus and the loss factor in the left figures are given, the complex wave number (real wavenumber and attenuation constant) is obtained using the direct formulas. On the other hand, in the inverse calculation, the viscoelastic data are calculated from the complex wave number using the inverse formulas. In the graph on the left side of the complex modulus, the inverse result is consistent with the direct result. Therefore, the inversion formulas can be considered valid. The formulas of the complex wave number from viscoelasticity and the formulas for their inversion are shown below Fig. 2.

(*) Similar relations hold for the flexural waves propagating in the viscoelastic beams and plates. We would like to discuss them on another occasion.

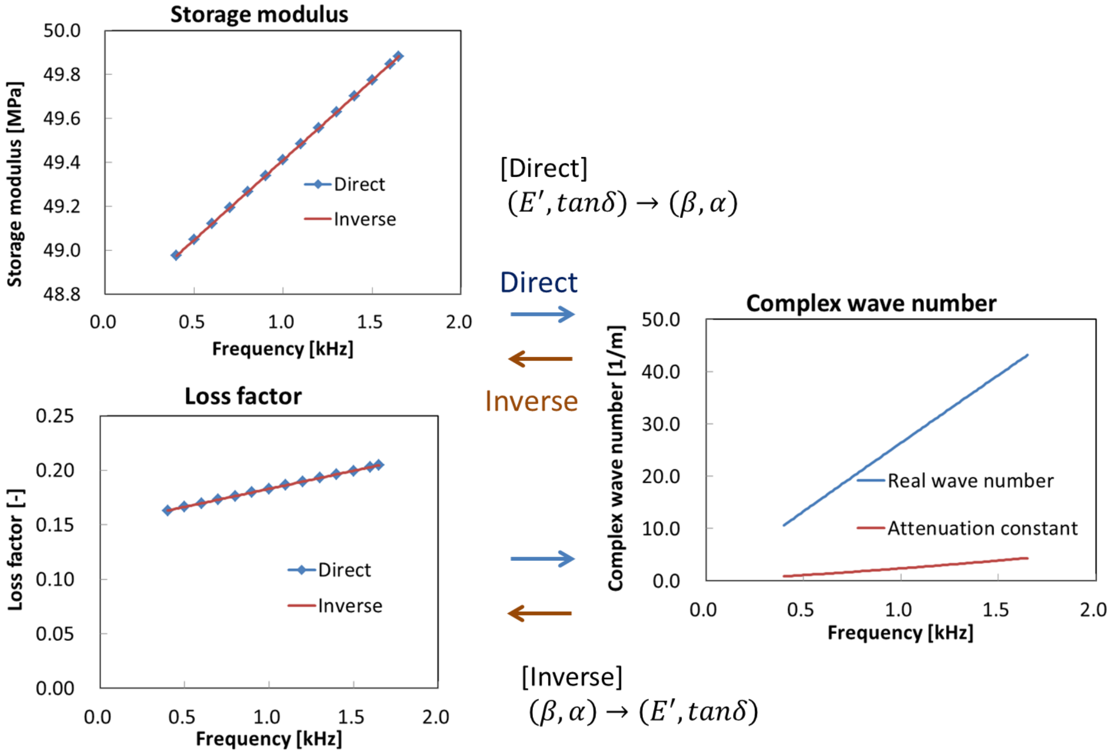

Fig.2. Direct and inverse calculations (Viscoelasticity to complex wave number)

[Formulas used in Fig.2]

Direct formulas (Eqs.(5) and (6))

$$\beta(\omega) = \omega \left[\frac{\rho}{2E'(\omega)}\right]^{\frac{1}{2}} \left[\frac{1}{(1+\tan^2\delta)^{1/2}} + \frac{1}{1+\tan^2\delta}\right]^{\frac{1}{2}}, \quad \text{(Real wave number [1/m])}$$

$$\alpha(\omega) = \omega \left[\frac{\rho}{2E'(\omega)}\right]^{\frac{1}{2}} \left[\frac{1}{(1+\tan^2\delta)^{1/2}} - \frac{1}{1+\tan^2\delta}\right]^{\frac{1}{2}} \quad \text{(Attenuation constant [1/m])}$$

Inverse formulas (Eqs.(B2)) For details, see Appendix A in [4].

$$\tan\delta = \left[\left(\frac{\beta^2+\alpha^2}{\beta^2-\alpha^2}\right)^2 - 1\right]^{1/2}, \quad \text{(Loss factor [-])}$$

$$E' = \frac{\rho\omega^2}{\beta^2+\alpha^2} \cdot \frac{1}{(1+\tan^2\delta)^{1/2}} = \rho\omega^2 \frac{\beta^2-\alpha^2}{(\beta^2+\alpha^2)^2} \quad \text{(Storage modulus [Pa])}$$

In Fig. 3, on the one hand, when the complex wave number is given as shown in the graph on the left side, the complex characteristic impedance of the material is calculated using the direct formulas. On the other hand, using the inverse formulas, the complex wave number (real wave number and attenuation constant) can be calculated from the complex characteristic impedance of the material (inverse calculations). In the graph on the left side of the complex wave number, the inverse result is consistent with the direct result. Therefore, the inversion formulas can be considered valid. The formulas for calculating the characteristic impedance from the complex wave number used in Fig. 3 and the formulas for their inversion are shown below the figure.

By continuing to use the formulas at the bottom of Fig. 2 and Fig. 3, it is possible to perform the direct and inverse calculations between viscoelasticity $(E', tan\delta)$ and complex characteristic impedance Z^*_{SP}.

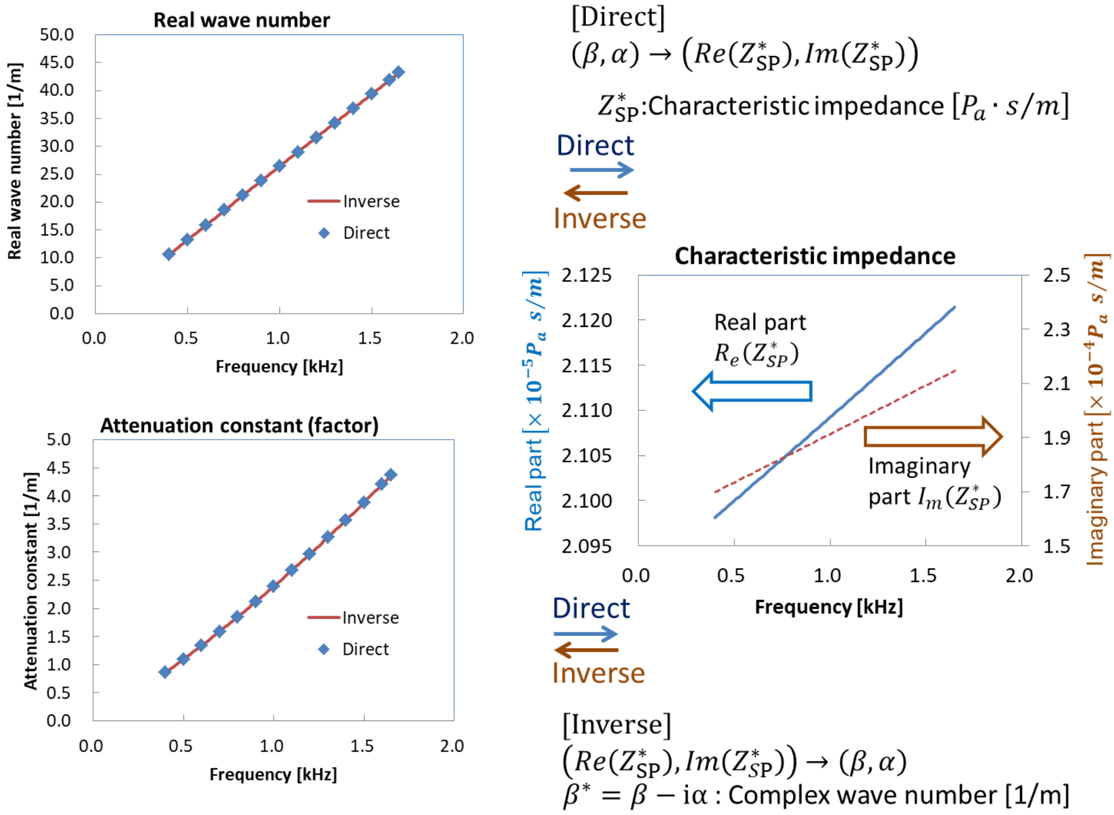

Fig.3. Direct and inverse calculations (Complex wave number to characteristic impedance)

[Formulas used in Fig.3]

Direct formulas (Eqs.(B3)) For details, see Appendix A in [4].

$Z^*_{SP}(\omega) = R_e(Z^*_{SP}) + iI_m(Z^*_{SP}),$ (Characteristic impedance of the specimen $[P_a\ s/m]$)

where

$$R_e(Z^*_{SP}) = \frac{\rho\omega\beta}{\beta^2+\alpha^2}\ ,I_m(Z^*_{SP}) = \frac{\rho\omega\alpha}{\beta^2+\alpha^2}\ ,i = \sqrt{-1}$$

Inverse formulas (Eqs.(B4)) For details, see Appendix A in [4].

$\beta^* = \beta - i\alpha$, (Complex wave number [1/m])

where

$$\beta = \frac{1}{1+[I_m(Z^*_{SP})/R_e(Z^*_{SP})]^2} \cdot \frac{\rho\omega}{R_e(Z^*_{SP})}\ ,\alpha = \frac{I_m(Z^*_{SP})/R_e(Z^*_{SP})}{1+[I_m(Z^*_{SP})/R_e(Z^*_{SP})]^2} \cdot \frac{\rho\omega}{R_e(Z^*_{SP})}$$

2.2 Estimation of the Acoustic Impedance Z^*_{23} as Viewed from the Left Side of the Specimen from the Acoustic Impedance Z^*_{tot}

When the acoustic impedance Z^*_{tot} of the whole system as viewed from the left end of Fig. 1 is obtained from the measurement, the acoustic impedance Z^*_{23} as viewed from the left end of the specimen is obtained as follows:

$$Z_{23}^{*} = Z_{Steel} \frac{\left(Z_{tot}^{*}/Z_{Steel}\right) + i\tan\left(\omega L_{Steel}/c_{Steel}\right)}{1 + i\left(Z_{tot}^{*}/Z_{Steel}\right)\tan\left(\omega L_{Steel}/c_{Steel}\right)} \quad . \tag{7}$$

(See Eq. (A1_2) in Appendix A)

The relationship between Z_{tot}^{*} and Z_{23}^{*} is shown in Fig. 4. As it is a simple relation, we do not show the numerical confirmation of Eq. (7) here.

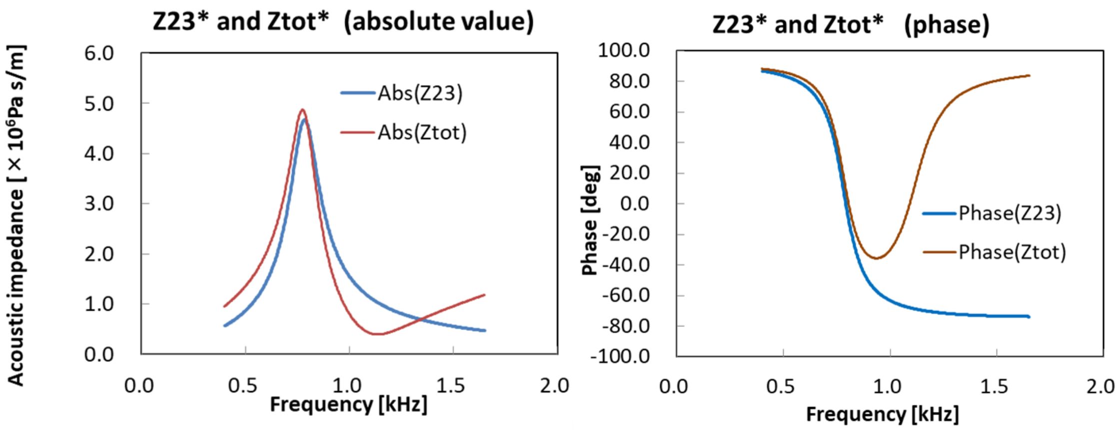

(For the physical properties and dimensions, see Appendix C.)

Fig.4 Acoustic impedance of the whole system and the specimen

(Concern)

When Z_{tot}^{*} and Z_{23}^{*} are expressed in the following form, it will be necessary to pay attention to the effect of poles:

$$\sum_{k}\left(c_k^{*} Z_k^{*} + d_k^{*} + \frac{a_k^{*}}{Z_k^{*} - b_k^{*}} \right) \quad . \tag{8}$$

2.3 Estimation of the Characteristic Impedance Z_{SP}^{*} of the Specimen from the Acoustic Impedance Z_{23}^{*}

When the acoustic impedance Z_{23}^{*} is given, the characteristic impedance Z_{sp}^{*} of the specimen is calculated by solving the quadratic equation (9a) of the complex coefficients. (See Eq.(A2_2) in Appendix A.) However, from the mechanical point of view, the real part of Z_{sp}^{*} is positive and the imaginary part is nonnegative (Eq. (9b)). Furthermore, the coefficient C_1^{*} in Eq. (9a) is a function of the real wave number β and the attenuation constant α in the specimen. β and α can be expressed as functions of Z_{sp}^{*} (Eq. (10)). Therefore, the iterative procedure through the under relaxation method was applied to the numerical calculation of Eqs. (9) to (10).

In the current inverse calculation, this procedure is the most complicated one.

(Quadratic equation of the complex coefficient on Z_{SP}^{*})

$$\left(Z_{SP}^{*}\right)^2 - C_1^{*} Z_{SP}^{*} - C_2^{*} = 0 ,$$

where

$$C_1^{*} = \left(Z_{23}^{*} - Z_{3b}^{*}\right)\coth\left[(\alpha + i\beta)L_{SP}\right] = \left(Z_{23}^{*} - Z_{3b}^{*}\right)\frac{\sinh\left(2\alpha L_{SP}\right) - i\sin\left(2\beta L_{SP}\right)}{\cosh\left(2\alpha L_{SP}\right) - \cos\left(2\beta L_{SP}\right)} ,$$

$$C_2^{*} = Z_{23}^{*} Z_{3b}^{*} \tag{9a}$$

Z_{3b}^{*} : The acoustic impedance viewed from the left end of the steel rod on the right side in Fig. 1 [$\mathrm{Pa}\cdot s/m$]

$$\mathrm{Re}\left(Z_{SP}^{*}\right) > 0 , \mathrm{Im}\left(Z_{SP}^{*}\right) \geq 0 \tag{9b}$$

$$\beta = \frac{1}{1+\left[\mathrm{Im}\left(Z_{SP}^{*}\right)/\mathrm{Re}\left(Z_{SP}^{*}\right)\right]^{2}} \cdot \frac{\rho\omega}{\mathrm{Re}\left(Z_{SP}^{*}\right)}, \quad \alpha = \frac{\mathrm{Im}\left(Z_{SP}^{*}\right)/\mathrm{Re}\left(Z_{SP}^{*}\right)}{1+\left[\mathrm{Im}\left(Z_{SP}^{*}\right)/\mathrm{Re}\left(Z_{SP}^{*}\right)\right]^{2}} \cdot \frac{\rho\omega}{\mathrm{Re}\left(Z_{SP}^{*}\right)} \tag{10}$$

(i.e., the real wave number and attenuation constant in the specimen, respectively)
(See Appendix B)

An outline of the direct and inverse calculations is shown in Fig. 5. Numerical examples are also attached to the figure. In Fig. 5(b), the characteristic impedances Z_{sp}^{*} from the direct and inverse calculations are consistent with each other. Furthermore,in Fig.5(a), the complex wave number β^{*} obtained through the iterative procedure is identical to that obtained from direct calculation. In Fig. 5, the lower limit of the frequency was set to 400 Hz. The calculation procedure of Fig. 5 is summarized below the figure.

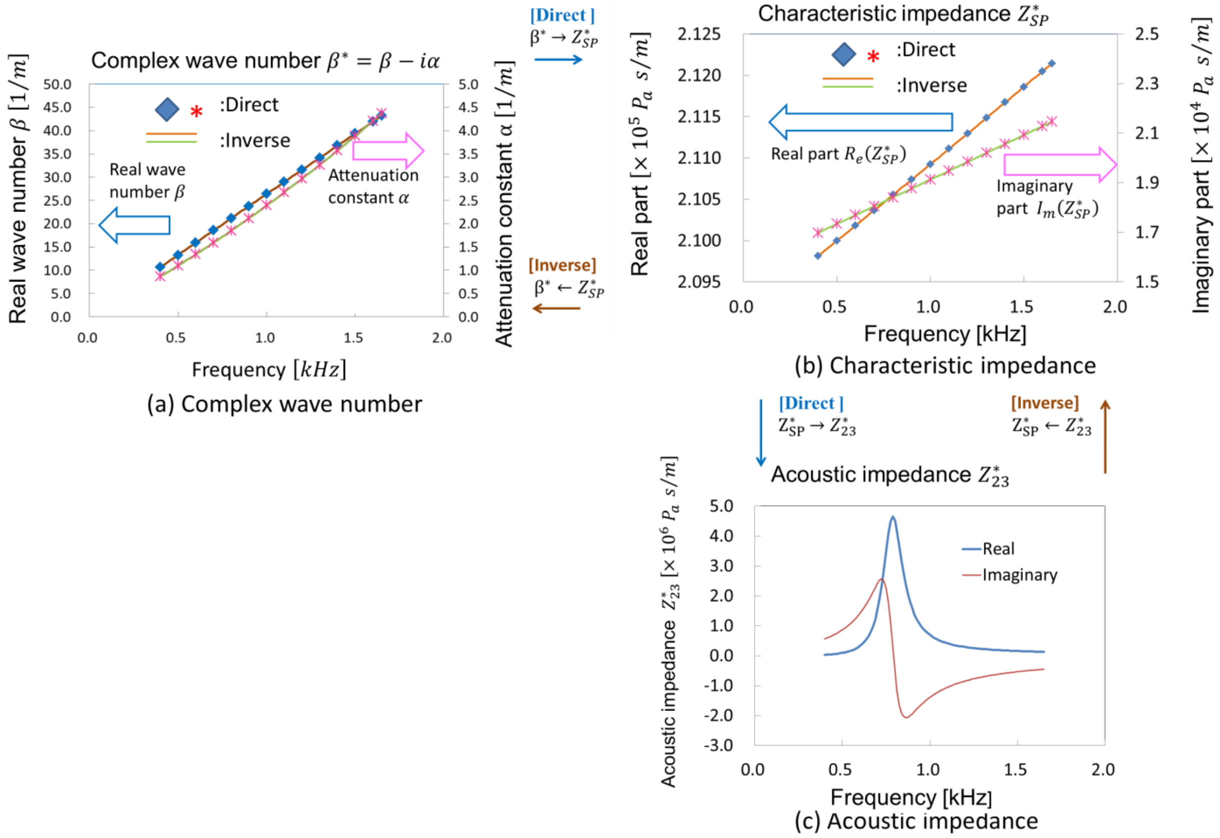

Fig.5. Direct and inverse calculations (Characteristic impedance Z_{SP}^{*} to the acoustic impedance Z_{23}^{*}, Frequency ≥ 400 Hz, Specimen: VC6400 in [1])
(See Eqs. (9) and (10) and Eqs. (A2_3)–(A2_7) in Appendix A)

[Formulas used in Fig.5]

Direct calculations in Fig.5 ($Z_{SP}^{*} \rightarrow Z_{23}^{*}$) (See Eq.(7) and Appendix B.)

$$Z_{23}^{*} = Z_{SP}^{*} \cdot \frac{coth[(\alpha + i\beta)L_{SP}] + (Z_{SP}^{*}/Z_{3}^{*})}{1 + (Z_{SP}^{*}/Z_{3}^{*})coth[(\alpha + i\beta)L_{SP}]},$$

(Acoustic impedance as viewed from the left end of the specimen $[P_a\, s/m]$)

where

$Z_{SP}^{*} = \rho\omega\,(\beta + i\alpha)/(\beta^{2} + \alpha^{2})$ (Characteristic impedance of the specimen$[P_a\, s/m]$),

$$\beta = \omega \left[\frac{\rho}{2E'(\omega)}\right]^{\frac{1}{2}} \left[\frac{1}{(1+\tan^2\delta)^{1/2}} + \frac{1}{1+\tan^2\delta}\right]^{\frac{1}{2}}$$ (Real wave number [1/m]),

$$\alpha = \omega \left[\frac{\rho}{2E'(\omega)}\right]^{\frac{1}{2}} \left[\frac{1}{(1+\tan^2\delta)^{1/2}} - \frac{1}{1+\tan^2\delta}\right]^{\frac{1}{2}}$$ (Attenuation constant [1/m])

Inverse (iterative) calculations in Fig.5 ($Z_{23}^* \rightarrow Z_{SP}^*$) (See Eqs.(9) and Appendix A.)

The quadratic equation (9a) is solved for the characteristic impedance Z_{SP}^* .

$$(Z_{SP}^*)^2 - C_1^* Z_{SP}^* - C_2^* = 0, Re(Z_{SP}^*) > 0, Im(Z_{SP}^*) \geq 0 \ ,$$

where

$$C_1^* = (Z_{23}^* - Z_{3b}^*) \frac{sinh(2\alpha L_{SP}) - i sin(2\beta L_{SP})}{cosh(2\alpha L_{SP}) - cos(2\beta L_{SP})} \ , C_2^* = Z_{23}^* Z_{3b}^*$$

The real wave number β and the attenuation constant α are calculated as functions of Z_{sp}^* as follows.

$$\beta = \frac{1}{1+[Im(Z_{SP}^*)/Re(Z_{SP}^*)]^2} \cdot \frac{\rho\omega}{Re(Z_{SP}^*)} \ , \alpha = \frac{Im(Z_{SP}^*)/Re(Z_{SP}^*)}{1+[Im(Z_{SP}^*)/Re(Z_{SP}^*)]^2} \cdot \frac{\rho\omega}{Re(Z_{SP}^*)}$$

Subsequently, we set the lower limit of the frequency in the inverse calculation to 200 Hz. At this time, the inverse analysis result of the characteristic impedance and the complex wave number diverged in the low-frequency region around 200 Hz (Fig. 6 and Fig. 7). The cause of divergence is still under consideration. We need to improve the iterative procedure and determine the convergence radius criteria.

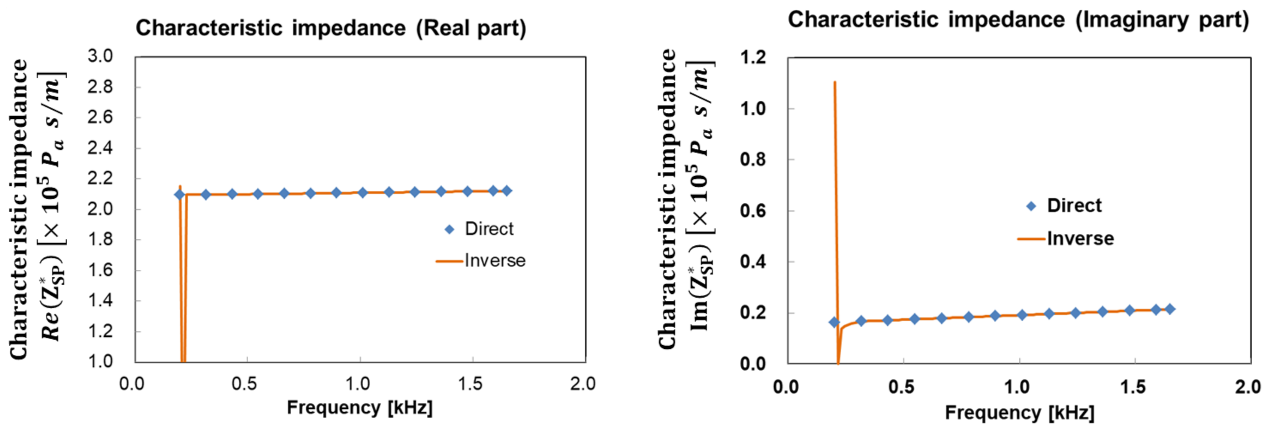

Fig.6. Divergence of the inverse calculation at the low frequency near 200 Hz
- Characteristic impedance -

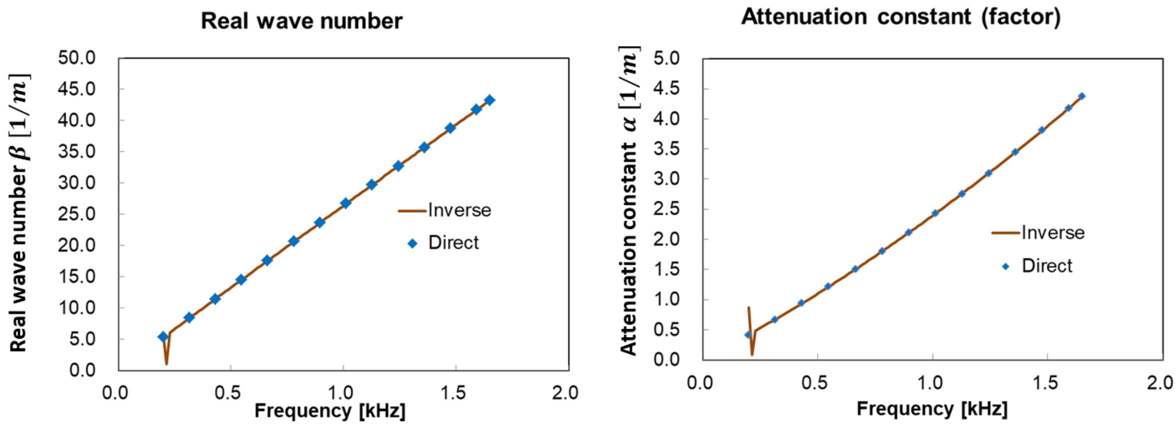

Fig. 7 Divergence of the inverse calculation at the low frequency near 200 Hz
- Complex wave number -

3. Conclusion

The acoustic impedance of the whole system can be calculated from the frequency response function (acceptance X / F). We investigate the inverse method for obtaining viscoelasticity when the acoustic impedance of the system is obtained. Each step of the inverse analysis traces the steps of direct analysis in reverse. We confirmed that the inversion results for each step reproduced the conditions of the direct calculations.

4. Future Tasks

In the inverse estimation of the characteristic impedance Z_{SP}^* from the acoustic impedance Z_{23}^* of the specimen, there was a divergence for the low-frequency range (200 Hz or less). We will develop a more stable inverse procedure for a wider frequency range.

Appendix A. Estimation of Viscoelasticity using Acoustic Impedance

In the case of a direct problem, the acoustic impedance of the whole system can be calculated from the viscoelastic data of the specimen through the following procedure.

(1) Viscoelasticity$(E', tan\delta)$→ (2) Characteristic impedance of the specimen Z_{SP}^* → (3) Acoustic impedance after the specimen Z_{23}^* → (4) Acoustic impedance of the whole system Z_{tot}^*

If the acoustic impedance Z_{tot}^* of the whole system is obtained from the frequency response function (such as acceptance X / F), can we identify viscoelasticity $(E', tan\delta)$? (This is the inverse problem.) Here, we consider the inverse analysis method step by step.

A1. Estimation of the Acoustic Impedance Z_{23}^* after the specimen from the Acoustic Impedance Z_{tot}^* of the Whole System

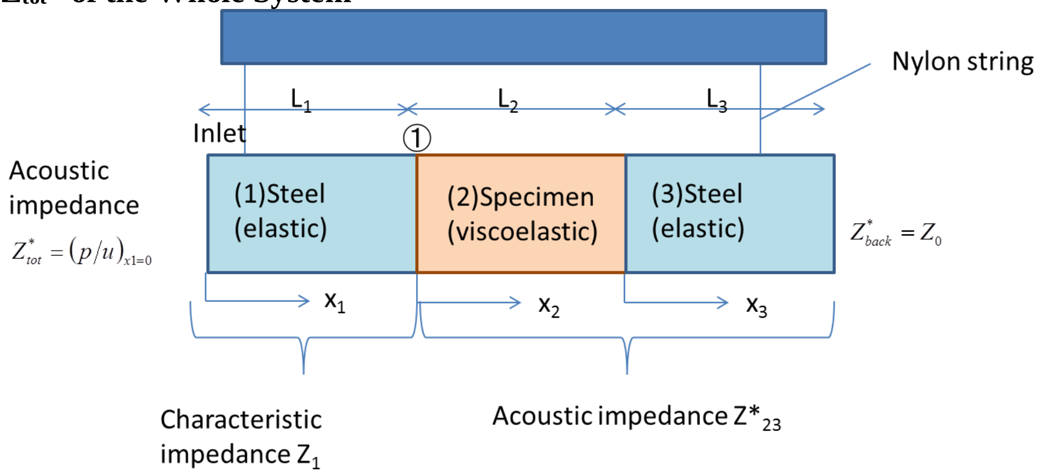

Fig.A1. Acoustic impedance of the system

First, the acoustic impedance Z_{tot}^* of the whole system as viewed from the left end of Fig. A1 can be expressed as follows (See Eq. (B1_7) in [4]):

$$\frac{Z_{tot}^*}{Z_{Steel}} = \frac{\left(Z_{23}^*/Z_{Steel}\right) + i\tan\left(\omega L_{Steel}/c_{Steel}\right)}{1 + i\left(Z_{23}^*/Z_{Steel}\right)\tan\left(\omega L_{Steel}/c_{Steel}\right)},$$

where

$$\beta(\omega) = \omega\left[\frac{\rho}{2E'(\omega)}\right]^{\frac{1}{2}}\left[\frac{1}{\left(1+\tan^2\delta\right)^{1/2}} + \frac{1}{1+\tan^2\delta}\right]^{\frac{1}{2}},$$

$$\alpha(\omega) = \omega\left[\frac{\rho}{2E'(\omega)}\right]^{\frac{1}{2}}\left[\frac{1}{\left(1+\tan^2\delta\right)^{1/2}} - \frac{1}{1+\tan^2\delta}\right]^{\frac{1}{2}},$$

$$Z_{Steel} = \rho_{Steel} c_{Steel},$$

$$c_{Steel} = \sqrt{\frac{E_{Steel}\left(1-\nu_{Steel}\right)}{\rho_{Steel}\left(1+\nu_{Steel}\right)\left(1-2\nu_{Steel}\right)}} \quad \text{(A1\_1)}$$

Eq. (A1_1) can be solved for Z_{23}^* as follows:

$$Z_{23}^* = Z_{Steel}\frac{\left(Z_{tot}^*/Z_{Steel}\right) + i\tan\left(\omega L_{Steel}/c_{Steel}\right)}{1 + i\left(Z_{tot}^*/Z_{Steel}\right)\tan\left(\omega L_{Steel}/c_{Steel}\right)}. \quad \text{(A1\_2)}$$

Thus, the acoustic impedance Z_{23}^* downstream from the specimen can be estimated using the measured value Z_{tot}^*.

A2. Estimation of the Characteristic Impedance Z_{sp}^* of the Specimen from the Acoustic Impedance Z_{23}^* Downstream from the Specimen

We apply Eq. (B1_7) in [4] (acoustic impedance of series rod) to the specimen (2) in Fig. A1. In this case, the acoustic impedance Z_{23}^* as viewed from the left side of the specimen can be expressed as follows:

$$\frac{Z_{23}^*}{Z_{SP}^*} = \frac{\coth\left[(\alpha + i\beta)L_{SP}\right] + \dfrac{Z_{SP}^*}{Z_{3b}^*}}{1 + \dfrac{Z_{SP}^*}{Z_{3b}^*}\coth\left[(\alpha + i\beta)L_{SP}\right]}, i = \sqrt{-1}, \quad \text{(A2\_1a)}$$

where

$$Z_{3b}^* = iZ_{Steel}\tan\left(\omega L_{Steel}/c_{Steel}\right) \quad \text{(A2\_1b)}$$

Z_{3b}^* is the acoustic impedance viewed from the left end of the steel rod (3) in Fig. A1 (See Eq. (C2_1) in [4]).

Eq. (A2_1 a) can be rewritten as follows:

$$\left(Z_{SP}^*\right)^2 - \left(Z_{23}^* - Z_{3b}^*\right)\coth\left[(\alpha + i\beta)L_{SP}\right]\cdot Z_{SP}^* - Z_{23}^* Z_{3b}^* = 0 \quad \text{(A2\_2)}$$

Assuming that the real wave number β and the attenuation constant α are known quantities, the above equation is a quadratic equation (A2_3) of the complex coefficients with respect to Z_{SP}^*.

$$\left(Z_{SP}^*\right)^2 - C_1^* Z_{SP}^* - C_2^* = 0,$$

where

$$C_1^* = \left(Z_{23}^* - Z_{3b}^*\right)\coth\left[(\alpha + i\beta)L_{SP}\right] = \left(Z_{23}^* - Z_{3b}^*\right)\frac{\sinh\left(2\alpha L_{SP}\right) - i\sin\left(2\beta L_{SP}\right)}{\cosh\left(2\alpha L_{SP}\right) - \cos\left(2\beta L_{SP}\right)}, \quad \text{(A2\_3)}$$

$$C_2^* = Z_{23}^* Z_{3b}^*$$

For the second equal sign of the expression on C_1^*, see (Note A1).

In Eq. (A2_3), the coefficient C_1^* is a function of the unknown complex wave number $\beta^* = \beta - i\alpha$. When the characteristic impedance Z_{SP}^* is obtained from Eq. (A2_3), the real wave number β and the attenuation constant α can be calculated using Eq. (A2_8) described later. Therefore, iterative calculations on Z_{SP}^*, β, and α are required.

If we regard Eq. (A2_3) as a quadratic equation of complex coefficients for Z_{SP}^*, its formal solution can be expressed as follows, as in the case of quadratic equations of real coefficients:

$$Z_{SP}^* = \frac{1}{2}\left[C_1^* \pm \sqrt{C_3^*}\right],$$

where (A2_4)

$$C_3^* = \left(C_1^*\right)^2 + 4C_2^*$$

However, care must be taken in handling the square root in Eq. (A2 _4) for complex coefficients. If the coefficient C_3^* is expressed in polar form as shown in Eq. (A2 _5), its square root can be expressed as Eq. (A2_6 a).

$$C_3^* = \left(C_1^*\right)^2 + 4C_2^* = r_3 \exp\left[i\left(\theta_3 + 2m\pi\right)\right], r_3 > 0, m = 0,1,2\cdots \quad \text{(A2\_5)}$$

Square Root of C_3^*

$$\left(C_3^*\right)^{1/2} = r_3^{1/2} \exp\left[i\left(\frac{\theta_3}{2} + m\pi\right)\right] \quad \text{(A2\_6a)}$$

Further,

$$-\left(C_3^*\right)^{1/2} = r_3^{1/2} \exp\left[i\left(\frac{\theta_3}{2} + (m+1)\pi\right)\right] \quad . \quad \text{(A2\_6b)}$$

From the mechanical meaning of the characteristic impedance, we must choose the roots that satisfy the following condition (Eq. (A2_7)):

$$\mathrm{Re}\left(Z_{SP}^*\right) > 0, \mathrm{Im}\left(Z_{SP}^*\right) \geq 0 \quad \text{(A2\_7)}$$

For calculation on Excel VBA, argument θ_3 and $\theta_3 + \pi$ of C_3^* are set as phase C 3 (1) and phase C 3 (2) as shown in Table A_ 1. Subsequently, we represent candidates of complex characteristic impedance Z_{SP}^* for two arguments as follows:

$$\mathrm{ReZ_{SPI}}(k) + i \cdot ImZ_{SPI}(k) \ , k = 1,2,3,4, i = \sqrt{-1}$$

We searched for the solutions satisfying Eq. (A2_7) from among these.

Table. A1. Procedure for obtaining a characteristic impedance satisfying the condition (A2_7) (Excel VBA)

```
    AL2 = 2 * alphZ23I(jfreq) * Lsp: BL2 = 2 * betaZ23I(jfreq) * Lsp
    eAL = Exp(AL2): snhAL = 0.5 * (eAL - 1 / eAL): cshAL = 0.5 * (eAL + 1 / eAL)
    snBL = Sin(BL2): csBL = Cos(BL2)
  'C1s  C1*
    Ar = ReZ23A(jfreq) - ReZ3(jfreq): Ai = ImZ23A(jfreq) - ImZ3(jfreq)
    Br = snhAL / (cshAL - csBL): Bi = -snBL / (cshAL - csBL)
    Re_AB = Ar * Br - Ai * Bi: Im_AB = Ai * Br + Ar * Bi ' Complex A*B
    ReCoef(1) = Re_AB: ImCoef(1) = Im_AB
  'C2s  C2*
    Ar = ReZ23A(jfreq): Ai = ImZ23A(jfreq)
    Br = ReZ3(jfreq): Bi = ImZ3(jfreq)
    Re_AB = Ar * Br - Ai * Bi: Im_AB = Ai * Br + Ar * Bi ' Complex A*B
    ReCoef(2) = Re_AB: ImCoef(2) = Im_AB
```

```
'C3s=C1s^2+4*C2s    C3*
  Ar = ReCoef(1): Ai = ImCoef(1): Br = Ar: Bi = Ai
  Re_AB = Ar * Br - Ai * Bi: Im_AB = Ai * Br + Ar * Bi ' Complex A*B
  ReCoef(3) = Re_AB + 4 * ReCoef(2): ImCoef(3) = Im_AB + 4 * ImCoef(2)
' abs(C3s) and Phase(C3s)
  absC3 = Sqr(ReCoef(3) ^ 2 + ImCoef(3) ^ 2)
  phaseC3(1) = Application.WorksheetFunction.Atan2(ReCoef(3), ImCoef(3))
  phaseC3(2) = phaseC3(1) + 2 * pi
'C4s & C5s=sqr(C3s) (Complex)    '(C3*)^1/2
  absC4 = Sqr(absC3)
  ReCoef(4) = absC4 * Cos(phaseC3(1) / 2): ImCoef(4) = absC4 * Sin(phaseC3(1) / 2)
  ReCoef(5) = absC4 * Cos(phaseC3(2) / 2): ImCoef(5) = absC4 * Sin(phaseC3(2) / 2)
'Candidates of Zsp
  ReZspI(1) = 0.5 * (ReCoef(1) + ReCoef(4)): ImZspI(1) = 0.5 * (ImCoef(1) + ImCoef(4))
  ReZspI(2) = 0.5 * (ReCoef(1) + ReCoef(5)): ImZspI(2) = 0.5 * (ImCoef(1) + ImCoef(5))
  ReZspI(3) = 0.5 * (ReCoef(1) - ReCoef(4)): ImZspI(3) = 0.5 * (ImCoef(1) - ImCoef(4))
  ReZspI(4) = 0.5 * (ReCoef(1) - ReCoef(5)): ImZspI(4) = 0.5 * (ImCoef(1) - ImCoef(5))
'Searching for ReZspI(k)>0 and ImZsp(k)>=0
    iSol = 0: iPsol = 0
  For i = 1 To 4 'Searching
      ReZspIP(i) = 0: ImZspIP(i) = 0 'Initial value ReZsp<=0 or ImZsp<0
    If ReZspI(i) > 0 And ImZspI(i) >= 0 Then    '*
      iPsol = i: iSol = iSol + 1 'iPsol :Candidate Number. Satisfying (A2_7)
      ReZspIP(iSol) = ReZspI(iPsol): ImZspIP(iSol) = ImZspI(iPsol)  ' Store variables that satisfy Re> 0, Im> = 0 in an array
      ReZspNew = ReZspIP(iSol): ImZspNew = ImZspIP(iSol) ' Variables that satisfy Re> 0, Im> = 0
    End If   ' * ReZspI(i) > 0 And ImZspI(i) >= 0 *
  Next i    'Searching
  nPsol = iSol    'nPsol : Number of nonnegative solutions
```

According to the fundamental theorem of algebra, the quadratic equation of the complex coefficients has two solutions in the complex number.

Let us assume that one complex number Z_{sp}^* such that the real part is not positive or the imaginary part is negative is obtained. At this time, if Z_{sp}^* that satisfies the condition (A2_7) is obtained, this is the only solution satisfying the condition (A2 _7).

Once the characteristic impedance Z_{sp}^* of the specimen is obtained, the complex wave number $\beta^* = \beta - i\alpha$ in the specimen can be obtained as follows.

Real Wave Number and Attenuation Constant of Longitudinal Wave in the Specimen

$$\beta = \frac{1}{1+\left[\mathrm{Im}\left(Z_{SP}^*\right)/\mathrm{Re}\left(Z_{SP}^*\right)\right]^2}\cdot\frac{\rho\omega}{\mathrm{Re}\left(Z_{SP}^*\right)},$$

$$\alpha = \frac{\mathrm{Im}\left(Z_{SP}^*\right)/\mathrm{Re}\left(Z_{SP}^*\right)}{1+\left[\mathrm{Im}\left(Z_{SP}^*\right)/\mathrm{Re}\left(Z_{SP}^*\right)\right]^2}\cdot\frac{\rho\omega}{\mathrm{Re}\left(Z_{SP}^*\right)} \tag{A2\_8}$$

(See Eqs.(B3) and (B4) in Appendix B. Here, $Z_C^* = Z_{SP}^*$.)

(Iterative Calculation)

In the quadratic equation (A2_3) of complex coefficients, the coefficient C_1^* is a function of the unknown quantities (the real wave number β and the attenuation constant α). Therefore, it is necessary to perform iterative calculation to simultaneously obtain Z_{sp}^*, real wave number β, and attenuation constant α.

We set $\mathrm{Re}(Z_{SP}^*)/Z_0$ and $\mathrm{Im}(Z_{SP}^*)/\mathrm{Re}(Z_{SP}^*)$ for the starting frequency as the initial value. For example, at 1600 Hz, $\mathrm{Re}(Z_{SP}^*)/Z_0$ is approximately 300 to 500 and $\mathrm{Im}(Z_{SP}^*)/\mathrm{Re}(Z_{SP}^*)$ is approximately 0.1.

Subsequently, we updated the real part and the imaginary part of the characteristic impedance to $\mathrm{Re}(Z_{SP}^{New*})$ and $\mathrm{Im}(Z_{SP}^{New*})$ using equations (A2_4) to (A2_8). Subsequently, the following relaxation calculation was applied to these updated values:

$$(\Delta L)_{ReZSP} = \ell_n(R_e(Z_{SP}^{New*}) + \varepsilon) - \ell_n(R_e(Z_{SP}^*) + \varepsilon),$$
$$(\Delta L)_{I_mZSP} = \ell_n(I_m(Z_{SP}^{New*}) + \varepsilon) - \ell_n(I_m(Z_{SP}^*) + \varepsilon),$$
$$\mathrm{Re}(Z_{SP}^*) \leftarrow \mathrm{Re}(Z_{SP}^*) \cdot exp(R_{elax} \cdot (\Delta L)_{ReZSP}) \quad ,$$
$$\mathrm{Im}(Z_{SP}^*) \leftarrow \mathrm{Im}(Z_{SP}^*) \cdot exp\left(R_{elax} \cdot (\Delta L)_{I_mZSP}\right) \quad , \qquad \text{(A2\_9a)}$$

$$\beta = \frac{1}{1+\left[\mathrm{Im}(Z_{SP}^*)/\mathrm{Re}(Z_{SP}^*)\right]^2} \cdot \frac{\rho\omega}{\mathrm{Re}(Z_{SP}^*)},$$
$$\alpha = \frac{\mathrm{Im}(Z_{SP}^*)/\mathrm{Re}(Z_{SP}^*)}{1+\left[\mathrm{Im}(Z_{SP}^*)/\mathrm{Re}(Z_{SP}^*)\right]^2} \cdot \frac{\rho\omega}{\mathrm{Re}(Z_{SP}^*)} \qquad \text{(A2\_9b)}$$

$0 < R_{elax} < 1$ Relaxation parameter, $0 < \varepsilon \ll 1$ Positive small number such as 10^{-10}

The numerical calculation procedure in this section is summarized in Fig. A2.

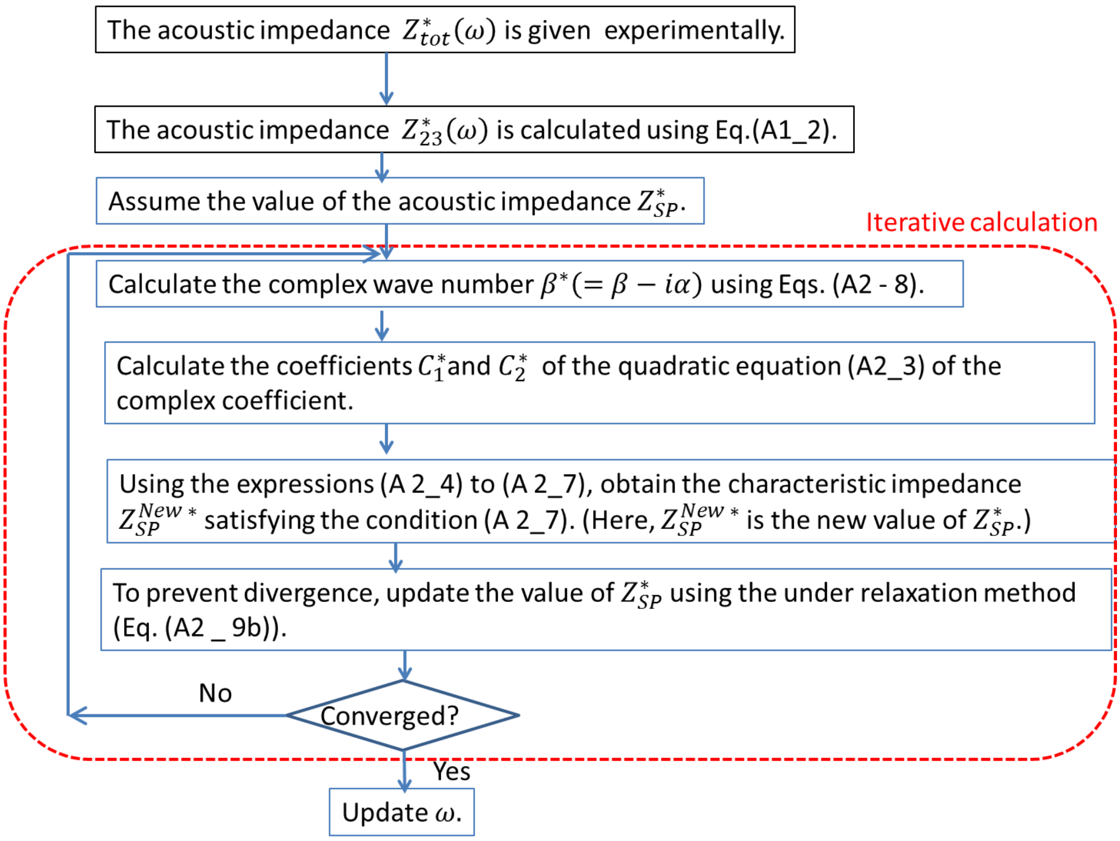

Fig. A2. Flow chart of the procedure in this section

(Note A1) Derivation of the second side of Eq.(A2 _3)

$$\coth[(\alpha+i\beta)L]$$
$$=\frac{\exp[(\alpha+i\beta)L]+\exp[-(\alpha+i\beta)L]}{\exp[(\alpha+i\beta)L]-\exp[-(\alpha+i\beta)L]} \quad \text{(a)}$$
$$=\frac{[\exp(\alpha L)+\exp(-\alpha L)]\cos(\beta L)+i[\exp(\alpha L)-\exp(-\alpha L)]\sin(\beta L)}{[\exp(\alpha L)-\exp(-\alpha L)]\cos(\beta L)+i[\exp(\alpha L)+\exp(-\alpha L)]\sin(\beta L)}$$

Multiply the numerator and denominator of the above equation by the following factor F, which is the conjugate complex number of the denominator.

$$F=[\exp(\alpha L)-\exp(-\alpha L)]\cos(\beta L)-i[\exp(\alpha L)+\exp(-\alpha L)]\sin(\beta L)$$

(Numerator) × F

$$\{[\exp(\alpha L)+\exp(-\alpha L)]\cos(\beta L)+i[\exp(\alpha L)-\exp(-\alpha L)]\sin(\beta L)\}$$
$$\times\{[\exp(\alpha L)-\exp(-\alpha L)]\cos(\beta L)-i[\exp(\alpha L)+\exp(-\alpha L)]\sin(\beta L)\}$$
$$=[\exp(\alpha L)+\exp(-\alpha L)][\exp(\alpha L)-\exp(-\alpha L)]\cos^2(\beta L)$$
$$+[\exp(\alpha L)-\exp(-\alpha L)][\exp(\alpha L)+\exp(-\alpha L)]\sin^2(\beta L)$$
$$+i[\exp(\alpha L)-\exp(-\alpha L)]^2\sin(\beta L)\cos(\beta L)$$
$$-i[\exp(\alpha L)+\exp(-\alpha L)]^2\sin(\beta L)\cos(\beta L)$$
$$=[\exp(2\alpha L)-\exp(-2\alpha L)]+i[-4\sin(\beta L)\cos(\beta L)]$$
$$=2\sinh(2\alpha L)-2i\sin(2\beta L)$$

(Denominator) × F

$$[\exp(\alpha L)-\exp(-\alpha L)]^2\cos^2(\beta L)+[\exp(\alpha L)+\exp(-\alpha L)]^2\sin^2(\beta L)$$
$$=[\exp(2\alpha L)+\exp(-2\alpha L)-2]\cos^2(\beta L)+[\exp(2\alpha L)+\exp(-2\alpha L)+2]\sin^2(\beta L)$$
$$=2\cosh(2\alpha L)-2\cos(2\beta L)$$

Therefore, the following relation is obtained:

$$\coth[(\alpha+i\beta)L]=\frac{\sinh(2\alpha L)-i\sin(2\beta L)}{\cosh(2\alpha L)-\cos(2\beta L)} \quad . \quad \text{(b)}$$

Appendix B. Relation between the Characteristic Impedance, Complex Wave Number, and Viscoelasticity

We present the relation between the characteristic impedance, complex wave number, and viscoelasticity derived in the previous studies [3],[4].

[Relation between the Viscoelasticity and Complex Wave Number]
(Direct)
Real Wave Number

$$\beta(\omega)=\omega\left[\frac{\rho}{2E'(\omega)}\right]^{\frac{1}{2}}\left[\frac{1}{(1+\tan^2\delta)^{1/2}}+\frac{1}{1+\tan^2\delta}\right]^{\frac{1}{2}} \quad \text{(B1a)}$$

Attenuation Constant (factor)

$$\alpha(\omega)=\omega\left[\frac{\rho}{2E'(\omega)}\right]^{\frac{1}{2}}\left[\frac{1}{\left(1+\tan^2\delta\right)^{1/2}}-\frac{1}{1+\tan^2\delta}\right]^{\frac{1}{2}} \qquad \text{(B1b)}$$

↔

(Inverse)

Loss Tangent (factor) and Storage Modulus

$$\tan\delta=\left[\left(\frac{\beta^2+\alpha^2}{\beta^2-\alpha^2}\right)^2-1\right]^{1/2},$$

$$E'=\frac{\rho\omega^2}{\beta^2+\alpha^2}\cdot\frac{1}{\left(1+\tan^2\delta\right)^{1/2}}=\rho\omega^2\frac{\beta^2-\alpha^2}{\left(\beta^2+\alpha^2\right)^2} \qquad \text{(B2)}$$

[Relation between the Characteristic Impedance and Complex Wave Number]

(Direct)

Complex Characteristic Impedance

$$Z^*_{SP}(\omega)=\mathrm{Re}\left(Z^*_{SP}\right)+i\,\mathrm{Im}\left(Z^*_{SP}\right),$$

where (B3)

$$\mathrm{Re}\left(Z^*_{SP}\right)=\frac{\rho\omega\beta}{\beta^2+\alpha^2},\ \mathrm{Im}\left(Z^*_{SP}\right)=\frac{\rho\omega\alpha}{\beta^2+\alpha^2},\ i=\sqrt{-1}$$

↔

(Inverse)

Real Wave Number and Attenuation Constant

$$\beta=\frac{1}{1+\left[\mathrm{Im}\left(Z^*_{SP}\right)/\mathrm{Re}\left(Z^*_{SP}\right)\right]^2}\cdot\frac{\rho\omega}{\mathrm{Re}\left(Z^*_{SP}\right)},$$

$$\alpha=\frac{\mathrm{Im}\left(Z^*_{SP}\right)/\mathrm{Re}\left(Z^*_{SP}\right)}{1+\left[\mathrm{Im}\left(Z^*_{SP}\right)/\mathrm{Re}\left(Z^*_{SP}\right)\right]^2}\cdot\frac{\rho\omega}{\mathrm{Re}\left(Z^*_{SP}\right)} \qquad \text{(B4)}$$

Appendix C. Physical Properties and Dimensions

The physical properties and dimensions used in this study are listed in Table C1. The data in this table are the values described in the paper of Policarpo et al. [1]. Here, the storage modulus and the loss factor are the results estimated via modal-based inverse analysis. The two frequencies correspond to the two natural frequencies obtained by changing the lengths of the steel rods at both ends. We used the value obtained via linear interpolation of the data listed in the table as a relation between viscoelasticity and frequency.

Table C1. Properties and size of the specimen (Specimen A)

[Conditions] (Steel)			
ρ_{Steel}	Mass density [kg/m^3]	7640	
E_{Steel}	Young's modulus [GPa]	205	
ν_{Steel}	Poisson's ratio [-]	0	(*1)
c_{Steel}	Phase velocity [m/s]	5180.0	
Z_{Steel}	Characteristic impedance [Pa・s/m]	3.958E+07	
(Specimen)	Cork A		(*2)
ρ	Mass density [kg/m^3]	893.0	
(Viscoelasticity vs. frequency)			(*3)
	E'	$tan\delta$	
Frequency (Hz)	Storage modulus [MPa]	Loss factor [-]	
159.7	48.8	0.155	
1124.0	49.5	0.187	
[Dimension] (Length)			
Steel	L_{Steel} [mm]	20.5	
Specimen	L_{SP} [mm]	12.8	
Total	$L_{tot} = L_{SP} + 2L_{Steel}$ [mm]	53.8	
(Cross sectional area)			
$A_{rea}[m^2]$	4.0E-03		

(*1) Varied in the range $0 \leq \nu_{Steel} < 0.5$
(*2) and (*3): Policarpo's data (for their cork VC6400)
(*3): Policarpo's modal inversion results

References

[1] H. Policarpo, M.M. Neves and N.M.M. Maia, "A simple method for the determination of the complex modulus of resilient materials using a longitudinally vibrating three-layer specimen," ***Journal of Sound and Vibration,*** Vol. 332, pp. 246-263, 2013.
[2] A. El Mouhtadi, J. Duclos and H. Duflo, "Experimental determination of plate parameters with an air coupled instrument," 6th Groupe de Recherche 2501 and 9th Anglo-French Physical Acoustics Joint Conference, ***Journal of Physics: Conference Series,*** Vol. 269, 0120054, 2011.
[3] R. Horiguchi, Y. Oda and T. Yamaguchi, "Propagation of stress waves in viscoelastic rods and plates," ***Journal of Technology and Social Science,*** Vol.2, No.1, pp.24–39, 2018.
[4] R. Horiguchi and T. Yamaguchi, "Propagation of stress waves in viscoelastic rods and plates (2) –Acoustic impedance of a viscoelastic rod: Validation with literature data," ***Journal of Technology and Social Science,*** Vol.2, No.3, 2018.